High energy particle excitations as a measure of electronic crosstalk in MODIS and VIIRS VIS/NIR bands

Kevin Twedt[a], Truman Wilson[a], and Xiaoxiong Xiong[b]

[a]Science Systems and Applications Inc., Lanham, MD 20706, USA
[b]Sciences and Exploration Directorate, NASA/GSFC, Greenbelt, MD 20771, USA

ABSTRACT

The MODIS instruments aboard the Terra and Aqua satellites and the VIIRS instruments aboard the SNPP and NOAA-20 satellites each contain several arrays of Si detectors that measure Earth-reflected radiance in the visible and near-infrared spectral range. Even in the absence of incident light, the Si detectors are occasionally excited by high energy charged particles that pass through the spacecraft. These particle radiation events are, fortunately, infrequent enough that they do not lead to significant degradation of the detectors and they do not have a significant impact on the Earth scene radiance images. On the other hand, they are frequent enough that the cumulative data from many years on orbit may provide valuable diagnostic information about the sensors. In this paper, we provide some basic statistics on the frequency and magnitude of the particle excitation events for MODIS and VIIRS and explore the usefulness of this data as a measure of electronic crosstalk. Large amounts of crosstalk can degrade the quality of the Earth images, so it is crucial to have methods to characterize and correct for it on-orbit, which has previously been done for MODIS using lunar image analysis. The particle excitations can manifest as single-pixel spikes in the otherwise dark space view background, which may be an ideal source for evaluating crosstalk. We derive crosstalk coefficients between the NIR band detectors of Terra MODIS, and compare them to coefficients previously derived from lunar observations. The same approach is applied to SNPP VIIRS, which does not show any significant electronic crosstalk. While the HgCdTe detectors used in the MODIS and VIIRS infrared bands can also be excited by particle radiation, the magnitudes of the excitations are much smaller compared to the Si detectors and in general are not large enough to be useful for examining crosstalk.

Keywords: MODIS, VIIRS, calibration, crosstalk

1. INTRODUCTION

The MODIS instruments aboard the Terra and Aqua satellites and the VIIRS instruments aboard the SNPP and NOAA-20 satellites are polar-orbiting multi-band scanning radiometers with similar design, covering the visible through infrared wavelengths and providing daily imagery of the globe for a wide range of scientific and environmental applications.[1] Like all space-based instruments, some amount of particle radiation from the low-Earth orbit environment can penetrate the instruments' shielding and cause anomalous signals, sensor degradation, or other problems. Fortunately, negative impacts from particle radiation on the operation and the imagery products over the lifetime of the MODIS and VIIRS instruments have been minimal, and therefore it has not been the subject of much study.

Still, the impacts of radiation are evident and need to be considered. For example, the day-night band (DNB) on VIIRS has much higher sensitivity than other MODIS and VIIRS bands and is designed for viewing very low radiance nighttime imagery in a panchromatic, visible to near infrared wavelength range. In its high-gain stage, the DNB has a twin-detector operation that is designed for the specific purpose of removing any "hot" radiation-excited pixels from the imagery.[2] Also, there is evidence that particle radiation is at least partially responsible for increases in electronic crosstalk that have degraded the performance of the Terra MODIS long-wave infrared (LWIR) bands.[3] Even in normal operation, particle radiation can, infrequently, cause isolated hot pixels to appear in the response of any of the detectors in the Si and HgCdTe detector arrays that make up all MODIS and VIIRS bands besides the DNB.

Further author information: Send correspondence to kevin.twedt@ssaihq.com

In this paper, we provide some basic characterization of how high energy particle radiation manifests in the signals of the MODIS and VIIRS detectors. Rather than focus on any detrimental effect of the radiation, we instead explore the usefulness of this data as a measure of electronic crosstalk. Large amounts of crosstalk can degrade the quality of the Earth images, so it is crucial to have methods to characterize and correct for it on-orbit. Previous on-orbit crosstalk characterization has been done extensively for MODIS[3–7] and VIIRS[8] using lunar image analysis. MODIS crosstalk has also been evaluated using the on-board spectro-radiometric calibration assembly.[9] In contrast to these optical sources, the high energy particle excitations can manifest as single-pixel spikes in the otherwise dark space view background, which may make them an ideal source for evaluating crosstalk.

In Section 2, we describe the nature of the particle excitation events and how they manifest in the MODIS and VIIRS data. We present examples and statistics of the excitation events over the mission and provide a basic description of the physics involved. We focus on results from Terra MODIS and SNPP VIIRS, though we expect that Aqua MODIS and NOAA-20 VIIRS have similar behavior. We also focus on the VIS/NIR bands which use Si detectors. While the HgCdTe detectors used for the infrared bands can also be excited by particle radiation, the magnitudes of the excitations are much smaller compared to the Si detectors and thus not as useful.

In Section 3, we use the excitation events in the VIS/NIR bands to search for and characterize any electronic crosstalk. Both MODIS instruments have shown evidence of electronic crosstalk in bands 1 (645 nm) and 2 (858 nm) from lunar image analysis.[6] We compare the particle excitation data to the previous lunar results and find good agreement between the two methods. The same approach is applied to SNPP VIIRS, which does not show any significant electronic crosstalk. In addition, we observe a previously unidentified crosstalk that occurs between neighboring detectors within a band for both MODIS and VIIRS across all VIS/NIR bands. The magnitude of this in-band crosstalk is small and its impact on MODIS and VIIRS data products should be negligible.

2. PARTICLE EXCITATION EVENTS

2.1 Event description

MODIS and VIIRS are both scanning radiometers with similar design. Within one scan of the primary scan mirror for MODIS, or the rotating telescope assembly (RTA) for VIIRS, data is collected from the Earth-view (EV) sector, a space-view port (SV), and on-board calibrators. At any time during data collection, for any of the data sectors, a large single pixel spike can occur in the data record even when viewing a dark scene. We understand these signal spikes to be caused by high energy particles, or cosmic rays, which are typically protons, interacting with the atoms in the Si detector and ultimately exciting a large number of conduction electrons which provide the signal. The interaction of the incident particle with the detector and the subsequent cascade happen on very fast timescales and appear as instantaneous events where only one frame or sample of data is affected. A schematic description of an example excitation event is shown in Fig. 1. In this simplified schematic of a single detector excitation, the incident particle undergoes a collision and excites a response in one detector on the MODIS NIR focal plane assembly (FPA), and then passes through the rest of the instrument harmlessly.

Figure 2 shows examples of data from the SV sector of VIIRS band M1 in the high gain stage for three single scans from January 13, 2021. The left panel shows the SV sector data for a typical scan, with a few DN random variation in the signal due to the instrument noise at zero signal level. The middle and right panels show two different examples of an excited pixel of two different magnitudes. In both cases, the event clearly affects only one isolated sample, with no impact on neighboring samples.

The magnitude of the particle excitation signal varies over a wide range and can be very large, covering the entire range of possible signal levels with varying probability. These excitations can occur in any data sector, potentially impacting the quality of the calibration data collection or the EV imagery. For the dark SV data sector and the calibration sectors, these outlier pixels are typically discarded and don't have any negative impact. For our analysis of these excitation events, we focus only on the SV sector data as the otherwise dark background signal provides a clear way to identify and separate out the pixels excited by particle radiation. In the following sub-sections, we analyze the distribution and character of these events to establish a baseline understanding of how the particle radiation manifests in the MODIS and VIIRS signals, before moving on in Section 3 to discuss electronic crosstalk.

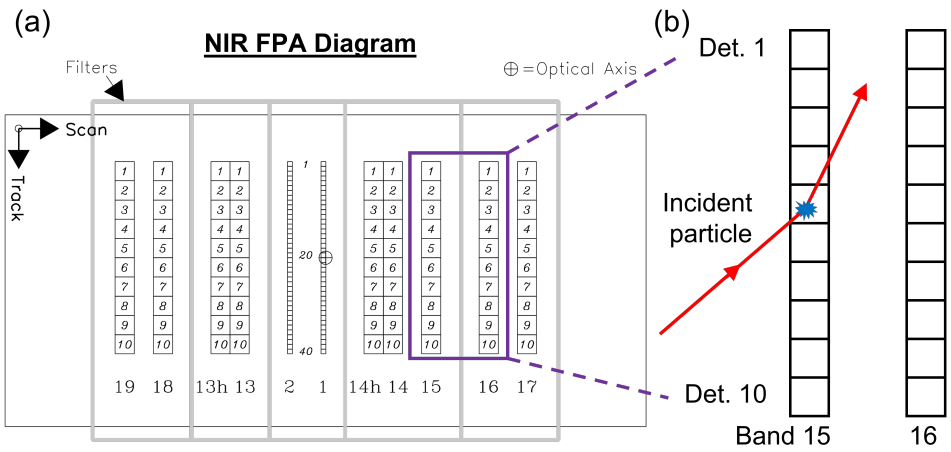

Figure 1. (a) Schematic of the MODIS NIR FPA. (b) Enlarged schematic of bands 15 and 16, which appear next to each other on the focal plane, with one of the band 15 detectors excited by an incident particle.

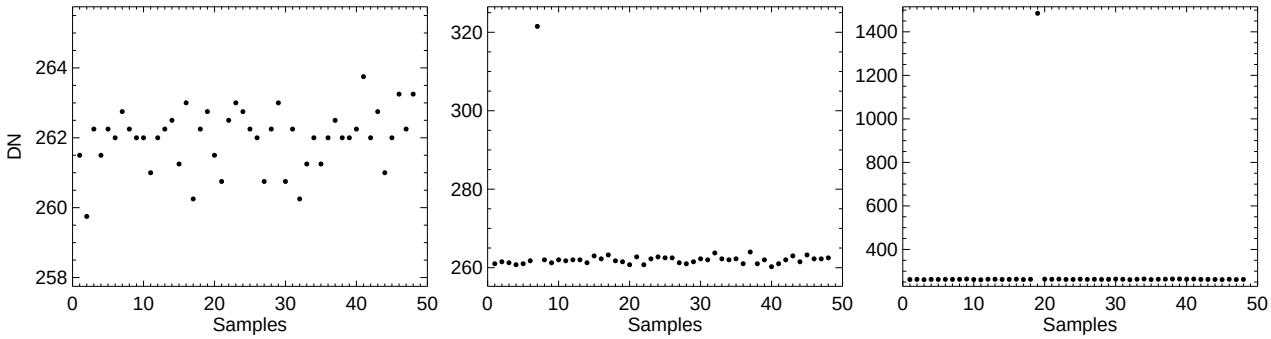

Figure 2. Examples of SV sector data for VIIRS band M1 detector 4 in the high gain stage from January 13, 2021: (left) Typical scan; (middle) Scan with an excitation 60 DN above the background; (right) Scan with an excitation 1223 DN above the background.

2.2 Frequency and distribution of events

To build a data set, we processed every scan of SV data in the month of January for each year of the Terra MODIS and SNPP VIIRS missions. We only process one month per year to limit the size of the data and processing time for this initial analysis. The choice of January is an arbitrary one and we don't expect there to be any meaningful variation in the results with time of year. In the processing, we search the SV signals of all detectors on every scan for any isolated single pixel excitation that is at least $dn > 100$ above the background level. For both MODIS and VIIRS, the raw digital signal output, DN, varies from 0 to 4095. Typical dark background signal levels are in the range of 50 to a few hundred, and the background-subtracted signal is represented by dn. The value of dn for the particle excitation pixel is taken as the SV DN of the excited pixel minus the mean SV DN of all remaining SV pixels in the same scan.

Figure 3 shows the number of excitation events recorded as a function of dn level for a few example bands of each instrument across the entire data set. The dn values are put into bins of width 100 and all detectors in each band are combined together to build the histograms. There is a very strong dependence on dn for all bands. While there are order 10^4 events recorded in the $dn = 100$ bin, there are only a handful of total events with $dn > 1000$ for most bands. More sensitive bands with high electronic gain register significantly more events, with SNPP VIIRS band M6 having the most overall. The VIIRS bands M1-M5 and M7 are dual gain bands. For half of the SV scans, these detectors are set to the high-gain stage and for the other half they are set to the low-gain stage. In the high-gain stage, these bands all have similar histograms as the one shown in Fig. 3

for M1, but very few events are registered when in the low-gain stage. For MODIS, the high-gain ocean bands 8-16 have the most events. Since the high energy particles directly excite electrons within the detectors, only the electronic components of the gain need to be considered; any differences in optical system gain or degradation of the optics over the missions are not relevant to the results.

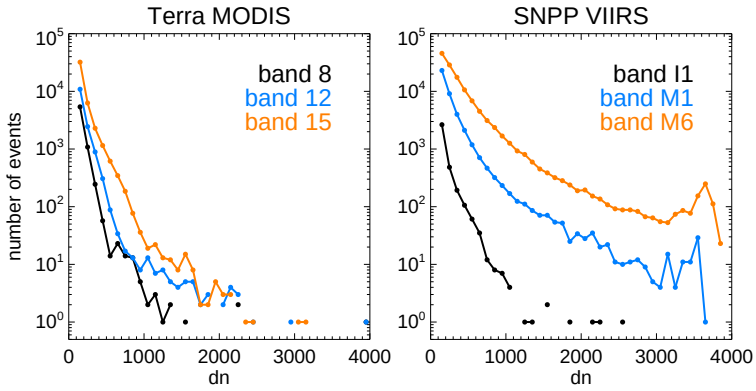

Figure 3. Event histogram as a function of *dn* for example bands of (left) Terra MODIS and (rigth) SNPP VIIRS.

We can also track how the number of excitation events changes in space and time. Within one day, the likelihood of particle excitation is significantly larger when the satellite is passing through the South Atlantic anomaly (SAA), a region of space where the particle radiation is known to be larger due to the shape of the Earth's magnetic field. Figure 4 shows a global map of the location of excitation events. Each blue dot represents one event and all events from Terra MODIS VIS/NIR bands from the January data throughout the mission are shown on the map. For regions where there are many overlapping points, a color scale is used to indicate the amount of overlap, shown as the relative event density in the figure. Clearly, there is a much higher density of events in the region of the SAA, which contains approximately 90% of all excitation events. Outside the SAA, the regions near the poles show slightly higher event density compared to other regions of the globe, because the polar orbit of the satellites causes them to spend more of their time over the polar regions.

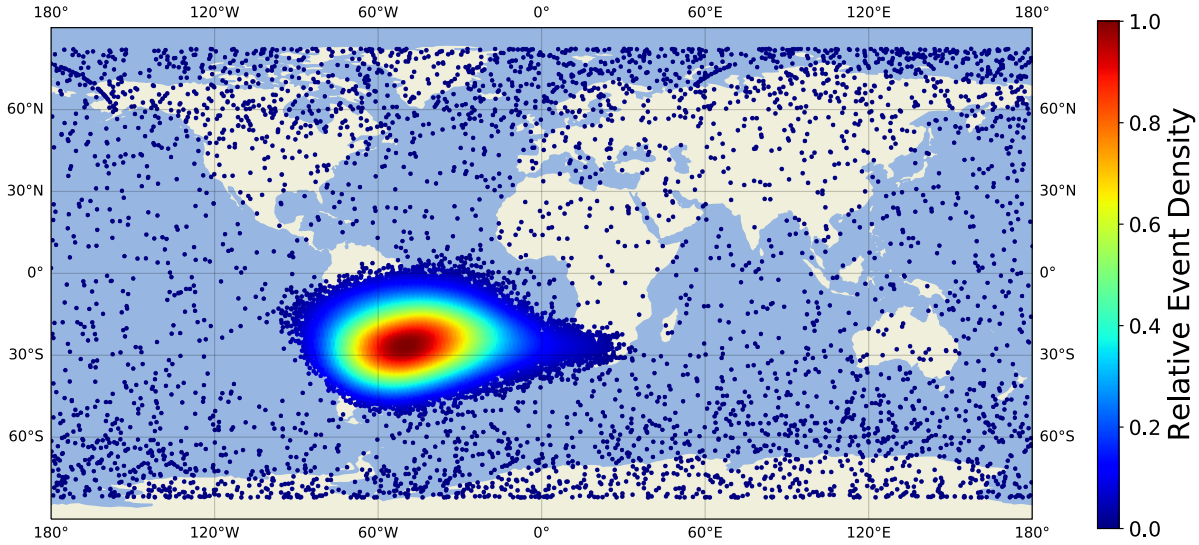

Figure 4. Global map showing location of excitation events from January of each year for all Terra MODIS VIS/NIR detectors.

Figure 5 shows the number of events detected per day for both Terra MODIS and SNPP VIIRS as a function

of time over the entire missions. In these plots, the total number of events recorded each day across all VIS/NIR bands are counted. Generally, the number of events recorded per day is relatively consistent, varying mostly within ±50 events from day to day. In rare instances, there are outlier days where an abnormally large number of spikes is recorded, and these can be associated with known events. For example, in January 2005 a series of large solar storms caused increased proton radiation at the Earth[10,11] and we see this as an abnormally large number of events in the Terra MODIS data from January 17-20, 2005, which are marked in the left panel of Fig. 5.

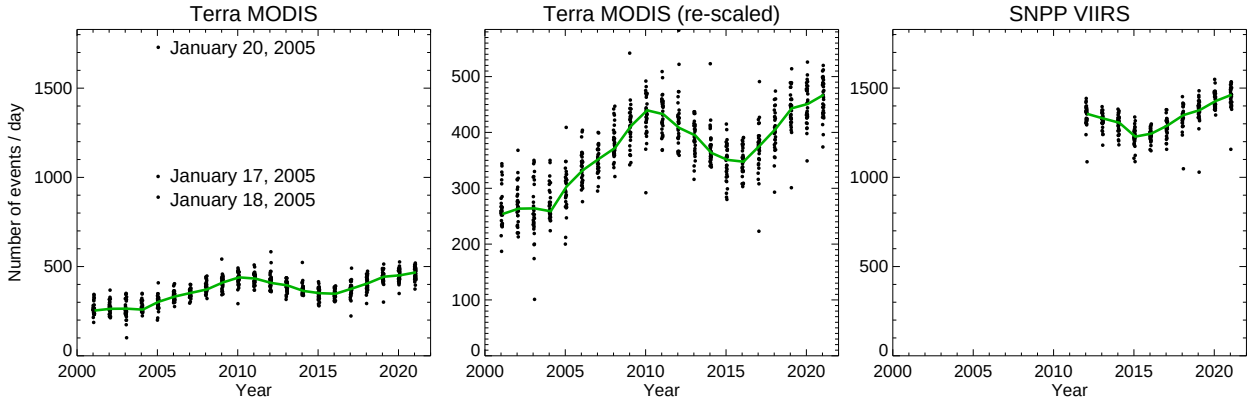

Figure 5. Number of events per day across all VIS/NIR bands. (left) Terra MODIS showing all data points including three outliers in January, 2005. (right) Terra MODIS re-scaled to exclude outliers and focus on the multi-year trend. (right) SNPP VIIRS showing all data points. Each black point is one day. The solid green lines are the yearly averages with outliers excluded.

From the middle and right panels of Fig. 5, there is a clear time trend to the average number of daily excitation events that follows the approximately 11-year solar cycle. For Terra MODIS, the event frequency is near a minimum in the first few years of the mission, grows steadily to a peak in 2010, falls to another minimum in 2016, and then rises again through 2021. Similarly, the SNPP VIIRS event frequency decreases from mission start through 2015 and then increases steadily through the current time. This behavior is expected, as the flux of protons observed in low Earth orbit is known to fluctuate with the solar cycle, with a maximum proton flux recorded near the time of the minimum in total solar irradiance.[12,13]

2.3 Secondary coincident excitations

While a large percentage of the events are truly single pixel excitations, where only one detector on the FPA has a *dn* above the background level for a given frame, there are also a large number of events where multiple pixels get excited at the same time. Figure 6 shows two examples of how a secondary, coincident excitation can occur. In the examples, a second detector is also excited either from a second collision of the original incident particle, or from a collision from a Si ion that was displaced during the initial collision. We call these coincident excitation events and they manifest as cases when multiple detectors show spikes in the SV signal at the same frame.

For both of the coincident excitation mechanisms shown in Fig. 6, the nearest neighboring detectors are the most likely to show coincident excitation and the likelihood of a coincident excitation decreases as the distance from the initial excitation detector increases. This spatial pattern is clearly observed in the SV data. To demonstrate, consider all of the excitation events where a single detector, MODIS band 15 detector 1 for example, has a large spike in the SV signal of at least $dn > 200$ and no other detector has a larger signal at the same frame. We count up the number of times when a coincident excitation of at least $dn > 25$ is seen in any other detector on the same FPA, and calculate the probability of coincident excitation for each detector. The result is shown in Fig. 7. In the MODIS example, detector 2 of band 15 has about a 20% chance of having an excitation when the primary excitation is in detector 1. The probability drops quickly as the physical separation of the detectors increases. The coincident excitations are not limited to the same band. For example, bands

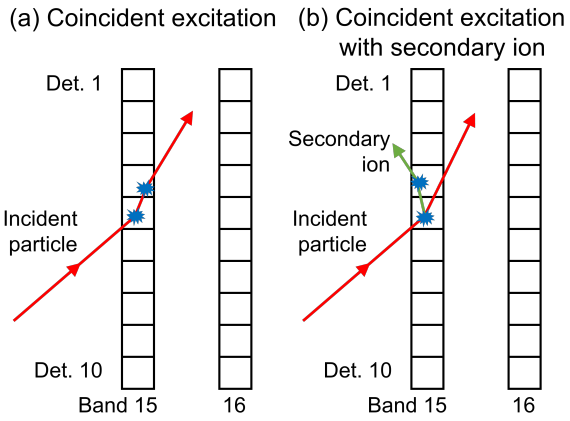

Figure 6. Examples of secondary, coincident excitations. Each panel shows the physical arrangement of the 10 detectors of MODIS NIR bands 15 and 16, which appear next to each other on the focal plane. (a) A coincident excitation with two neighboring detectors excited directly by the incident particle. (b) A coincident excitation where a secondary ion is generated in the primary collision and leads to the excitation of a neighboring detector.

14 and 16 neighbor band 15 on the MODIS NIR FPA (Fig. 1), spaced by -2.5 and 3 positions along scan, respectively, relative to band 15. The detectors in these bands that are nearest to band 15 detector 1 also see a notable probability of coincident excitation. For detectors that are 2 to 4 positions away from band 15 detector 1, including detectors 3-5 of band 15 and detectors 1-4 of bands 14h and 16, the probability of coincident excitation is around 1%. However, band 13, which is located on the opposite side of the FPA from band 15, 10.5 positions away, has almost no coincident excitations.

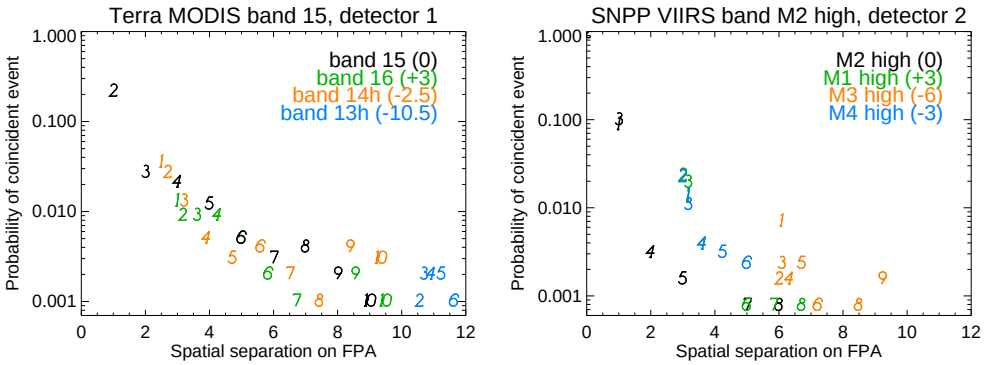

Figure 7. Probability of coincident excitations for a primary excitation in (left) Terra MODIS band 15 detector 1 and (right) SNPP VIIRS band M2 high gain detector 2. Each numbered symbol represents the detector number within each band. In the legends, the numbers in parentheses are the distance along-scan of each band relative to the sending band detector.

A similar spatial pattern is seen in VIIRS, with the example of band M2 detector 2 shown in Fig. 7. For VIIRS, the probability of coincident excitation is slightly lower than MODIS and drops off more quickly for detectors within a band. Interestingly, the probability is higher for detectors in neighboring bands of the same distance - e.g. detector 2 of bands M1 and M4 are separated by three positions along scan relative to the primary excitation in detector 2 of band M2, but they have notably higher probability compared to detector 5 of band M2, separated by three positions along track. The reason for this along-scan vs along-track difference is not clear, though it likely has to do with the exact physical properties and dimensions of the FPA. For both MODIS and VIIRS, the exact probabilities change if we adjust the thresholds for what counts as a primary excitation and what counts as a coincident excitation, set at $dn > 200$ and $dn > 25$, respectively, in this example. Regardless

of the choice, the general pattern of sharply reduced probability with increased physical distance is consistent across all bands and detectors of both instruments.

The schematics in Fig. 1 and Fig. 6 are very simplified pictures of the underlying physics. In reality, there are multiple mechanisms through which a high energy particle traveling through the instrument can transfer energy into the detectors. Any initial excitation could cause excitation of large numbers of electrons as well as the displacement of one or multiple Si ions in a detector and a cascade of collisions follows. The probability of excitation and the spatial extent of the cascade depend on the initial particle energy as well as the physical properties of the FPA.[14]

All of the evidence we have presented in this section, including the distribution of events in space and time and the correlation of signals in neighboring detectors, matches our expectations for the behavior of proton radiation in the low-Earth orbit environment. This supports the conclusion that at least the large majority of the isolated excited pixels observed in the SV sector data can be attributed to high energy particle excitations. In the following section, we study the usefulness of this data as a probe to characterize electronic crosstalk between detectors.

3. ELECTRONIC CROSSTALK

3.1 MODIS NIR band crosstalk

Crosstalk has been a concern since the very beginning of the Terra MODIS mission, with detectors in several bands showing evidence of optical and/or electronic crosstalk.[15,16] The most successful means for characterizing electronic crosstalk on-orbit has been through analysis of lunar image data.[3–7] The Moon is observed through the SV port and covers several pixels on the MODIS or VIIRS image. The spatial separation of the bands on the FPA means that detectors in different bands see the Moon at different times. Electronic crosstalk between detectors in different bands manifests as the presence of spatially separated ghost images of the Moon. The position and magnitude of these ghost images is analyzed to determine the bands and detectors that send and receive crosstalk to each other and to derive crosstalk correlation coefficients. The application of these Moon-derived coefficients to the EV sector data has been highly successful at improving the quality and accuracy of the imagery, most dramatically for the LWIR bands 27-30 of Terra MODIS in recent years.[3]

For the bands on the NIR FPA, electronic crosstalk exists in the bands 1 and 2 signals (250 m nadir resolution with 40 detectors per band) from the sending bands 13-19 (1 km nadir resolution with 10 detectors per band). The pattern of electronic crosstalk is related to the timing of the analog readout channels in the MODIS electronics. Figure 8 top panel shows a schematic of the analog readout sampling order for band 2 and bands 16 and 15, which are read out at the same time. Each receiving detector in band 2 receives crosstalk from up to two 1-km band detectors that are read out at nearly the same time. Three patterns of crosstalk were identified in the lunar analysis depending on how the 250-m band detectors sampling aligns with the 1-km detector sampling, with the detectors that temporally align with the beginning or end of 1-km detector arrays showing different behavior.[6] The three cases are represented by the red, green, and blue colors in the schematic in Fig. 8.

We observe all of the same crosstalk patterns in the particle excitation data. The bottom panel of Fig. 8 shows the receiving *dn* for band 2 detector 17, which receives crosstalk from sending detectors 9 and 10 of band 15. Each blue point corresponds to an individual particle excitation in the sending detector over the full data set (January data over full Terra mission). Only excitations with sending $dn > 200$ are shown and we have excluded all events that had any coincident excitation with $dn > 25$ to ensure that we focus only on single excitation events for the cleanest analysis. In both cases, there is a clear crosstalk effect which is well described by a quadratic fit. Similar results are found for other detector pairs, and the crosstalk correlation can be either positive or negative, as was also found in the lunar analysis.[6]

The magnitude of the observed crosstalk is also in good agreement with the lunar measurements. Figure 9 shows the receiving vs sending *dn* signals for two example detector pairs for a lunar observation compared to the particle excitation data. The receiving detectors are band 2 detectors 19 and 30, which have the most significant crosstalk contamination among the band 2 detectors. The red points are all taken from a single lunar calibration, combining data from multiple frames and scans. The black points are from the particle excitation data over the full data set. Clearly, the two independent data sources are in excellent agreement with each other. The particle

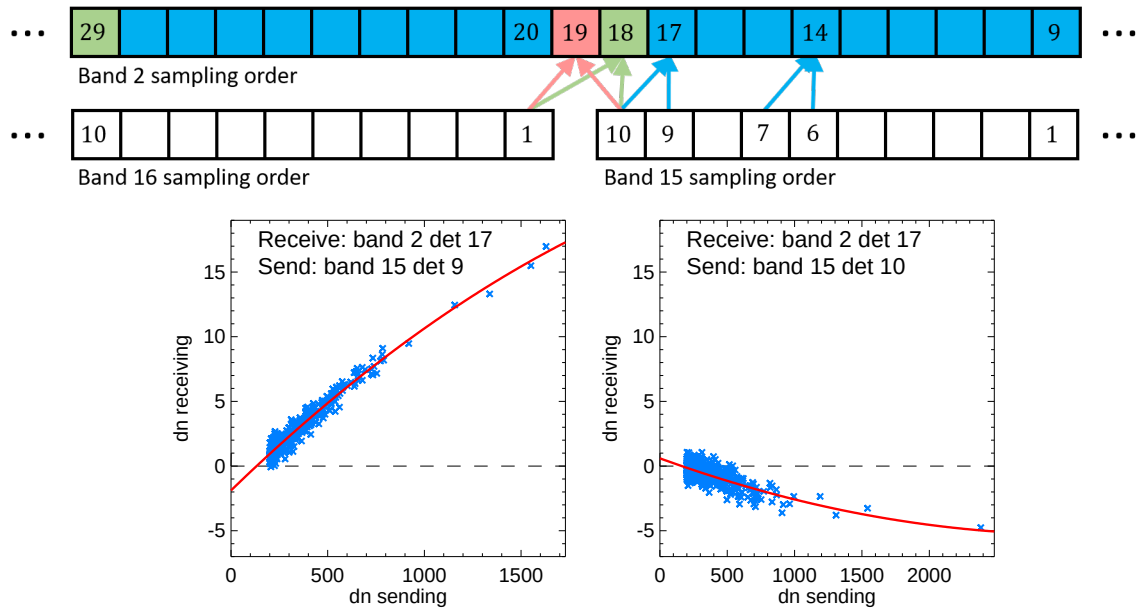

Figure 8. Examples of electronic crosstalk received in band 2. (top) Schematic of analog detector readout for detectors in bands 2, 16, and 15. Different patterns of crosstalk for a receiving detector are shown in the red, green, and blue colors. (bottom) Examples of receiving signal for band 2 detector 17 receiving crosstalk from sending detectors 9 and 10 of band 15. Blue points are individual particle excitation events and red lines are quadratic fits.

excitation data are heavily bunched at low dn values, with only a handful of events that have $dn > 1000$, whereas the lunar data provide much better coverage over the full range of sending dn. Despite the relative dearth of data in the high signal range, this analysis proves that the particle excitation events can be used to reliably derive crosstalk coefficients that agree with those from the well-established lunar methodology.

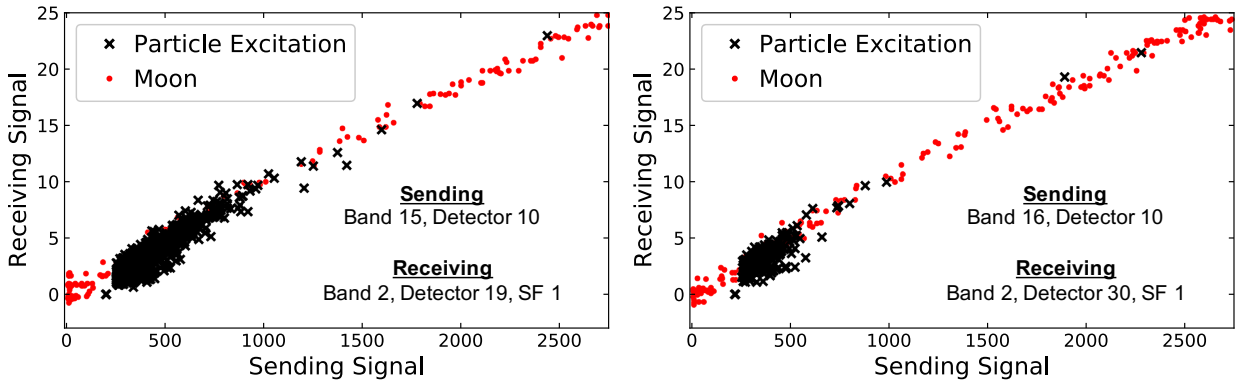

Figure 9. Receiving vs sending dn from a lunar observation compared to the particle excitation data for (left) band 15 detector 10 sending to band 2 detector 19 and (right) band 16 detector 10 sending to band 2 detector 30.

3.2 MODIS in-band crosstalk

In addition to the crosstalk received in the 250 m bands, we are also able to identify an in-band crosstalk which occurs between neighboring detectors within the same band. For an excitation event in detector N, a correlated crosstalk signal is observed in detector $N-1$. The identification of this crosstalk can be understood by examining

an example case shown in Fig. 10 with Terra MODIS band 15 detector 5 as the sending detector. For detector 3 ($N-2$), the signal level is consistently zero and there is no evidence of crosstalk. For detector 6 ($N+1$), the large majority of the data points have dn values around zero, with no indication of crosstalk, but there are also many points with larger signal levels where the receiving signal in detector 6 appears to be completely uncorrelated with the sending signal from detector 5. These are coincident excitation events. As we discussed in Sec. 2.3, up to 20% of the time that there is a primary excitation in detector 5, there is also a coincident excitation in the nearest neighbor detectors within the same band. The magnitude of the coincident excitations in detector 6 vary over a wide range, and in fact there are many more above the scale of the plot in Fig. 10. To analyze the trend without the influence of these coincident excitations, we fit the data using a linear fit with a repeated outlier rejection. After the initial fit, any data points more than three standard deviations from the fit line are counted as outliers and removed from the data set. The remaining data are re-fit and the process is repeated until no outliers remain. The blue points in Fig. 10 are the data remaining after the outlier rejection and the red line is the final fit; the green points are those identified as outliers. For receiving detector 6, there is clearly no correlated crosstalk present, and only the uncorrelated coincident excitations appear as positive signal.

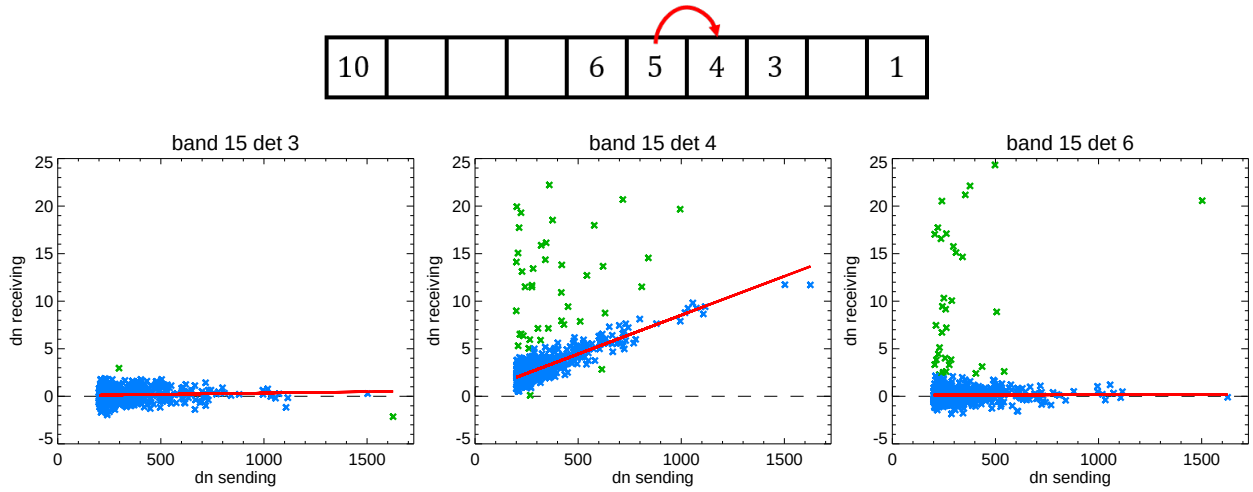

Figure 10. (top) Schematic of in-band crosstalk for Terra MODIS band 15 with detector 5 sending to detector 4. (bottom) Examples of receiving detector signals in Terra MODIS band 15 detectors 3 ($N-2$), 4 ($N-1$), and 6 ($N+1$), with the sending signal in detector 5. In all three panels, the red line is the result of a linear fit to the data points after a repeated outlier rejection. Each symbol represents one excitation event that occurred with $dn > 200$ in band 15 detector 5. Blue symbols are those points used in the final fit; green symbols are those identified as outliers, most of which are attributed to uncorrelated coincident excitations.

Lastly, we examine the signal in receiving detector 4 ($N-1$) in Fig. 10. In this case, there are again a large number of coincident excitations that appear as uncorrelated signal. But, there is also a very clear positive correlated crosstalk with the large majority of points falling along a linear trend line with a slope of about 0.008, or 0.8%.

The same behavior is observed for all of the detectors in band 15, with the exception of the edge detector. For detector 10, there is no crosstalk observed, as there is no $N+1$ detector to send it. The in-band crosstalk behavior is not limited to band 15, but is also observed in all detectors of bands 8-16, with nearly the same properties and magnitude. The magnitudes of the slope (receiving dn over sending dn) are in the range of 0.005 to 0.01 and the behavior appears to be stable in time. For bands 1-4 and 17-19, there are fewer events with large excitation signal, due to the lower gain of these bands, making any crosstalk harder to identify, so it is unclear whether or not the same type of in-band crosstalk exists for these bands. Like other MODIS crosstalk cases, the in-band crosstalk may also be linked to the analog readout timing, as shown in the schematic at the top of Fig. 10. In the analog readout, detector 10 of the 1-km bands is read first and the other detectors follow in order, so the detector receiving the crosstalk is the one read out immediately following the detector sending the crosstalk.

Notably, this in-band "previous detector" crosstalk has not been identified before. The lack of spatial separation between the sending and receiving detectors on the FPA makes it difficult to separate the signals in the lunar images. This demonstrates one of the main advantages to having a truly single-pixel excitation signal. While crosstalk in general has been a major concern for Terra MODIS, the in-band crosstalk should not have any major negative impact on the calibration or Earth-scene imagery. The coefficients are relatively small and neighboring detectors within the same band typically see very similar scenes and have nearly identical gain. Finally, we note that the in-band detector crosstalk does not extend to the case where detector 1 of any band sends crosstalk to detector 10 of the band that is subsequently read out on the same analog channel. Some infrared MODIS bands have significant crosstalk between the edge detectors (e.g. 10 sending to 1) of temporally neighboring bands on the analog readout, but this is not seen in any of the VIS/NIR bands.[3,6,7]

3.3 VIIRS in-band crosstalk

Previous studies of crosstalk in SNPP VIIRS from lunar image analysis did not find any significant crosstalk. Very small crosstalk coefficients were measured between some IR band detectors, but no detectable crosstalk was found in any of the VIS/NIR bands.[8]

From our particle event analysis, we also do not find any major crosstalk between VIS/NIR detectors. The one exception is that we again see a small but clear crosstalk from detector N to detector $N-1$ within the same band. An example of this is shown in Fig. 11 for band M1 high gain detector 8 as the sending detector, following the same analysis used for MODIS in Fig. 10. Once again, both the $N-1$ and $N+1$ detectors (detectors 7 and 9 in this example) have may data points with positive signal uncorrelated with the sending signal, which we attribute to uncorrelated coincident excitations, but only the $N-1$ detector shows any correlated crosstalk with the sending signal. In contrast to MODIS, the in-band crosstalk for VIIRS has a negative correlation. The magnitude is also smaller compared to MODIS, with a coefficient (slope) of -0.0013 (or -0.13%) in this example. Similar to MODIS, this crosstalk is observed for all VIS/NIR detectors in VIIRS, except for the edge detectors of each band. The only difference in behavior is for bands I1 and I2, which are higher resolution imagery bands with 375 m nadir spatial resolution compared to the 750 m resolution of the M bands. For excitations in a I-band sending detector N, a crosstalk is observed in receiving detector $N-2$ instead of $N-1$ and is isolated per sub-sample. This is because the I-band detectors are split into even and odd detectors and split by sub-sample when they are read out. So in terms of the analog readout, the detector receiving the crosstalk ($N-2$) is still the detector read out immediately following the sending detector. This strengthens the evidence that the in-band crosstalk is indeed related to the analog readout electronics and not the physical position on the FPA. Across all of the VIS/NIR bands, the magnitude of the in-band crosstalk is fairly consistent, with coefficients ranging from about -0.001 to -0.002. The existence of in-band crosstalk is especially notable for SNPP VIIRS, since no other crosstalk has been previously found from on-orbit analyses in any of the VIS/NIR bands. Fortunately, the magnitude is small enough that any impact on the calibration data or Earth imagery should be negligible.

4. SUMMARY

In summary, this paper presents a characterization of single pixel excitation events caused by particle radiation incident on the MODIS and VIIRS instruments. We find the distribution of events in space, time, and signal level to match the expectations for the behavior of proton radiation in low Earth orbit. We also find that the events which have multiple detectors excited at the same time have a clear spatial pattern that matches our expectations. We use the accumulated data over the Terra MODIS and SNPP VIIRS missions to show that the particle excitations can be used as a diagnostic tool to accurately measure electronic crosstalk between VIS/NIR band detectors. The derived crosstalk coefficients for Terra MODIS NIR band detectors agree well with the coefficients from the well-established lunar methodology.

One advantage of the particle excitation methodology is that the data is collected automatically, without the need for any special calibration procedure or spacecraft maneuver. Another advantage is the single-pixel nature of the excitations, which provides ideal isolation of sending and receiving signals. The single-pixel excitation allows us to observe crosstalk between neighboring detectors within the same band, which had not been previously seen in the lunar analyses. The in-band crosstalk exists for both MODIS and VIIRS, but the magnitudes are small - up to 1% for MODIS and 0.2% for VIIRS - and the crosstalk should have minimal impact on the accuracy

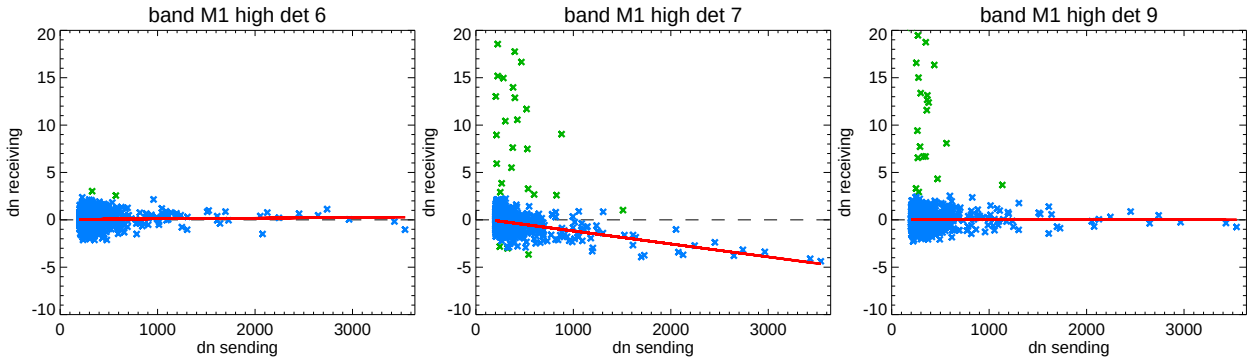

Figure 11. Examples of receiving detector signals in SNPP VIIRS band M1 detectors 6 ($N-2$), 7 ($N-1$), and 9 ($N+1$), with the sending signal in detector 8. In all three panels, the red line is the result of a linear fit to the data points after a repeated outlier rejection. Each symbol represents one excitation event that occurred with $dn > 200$ in band M1 detector 5. Only data from high gain scans are included. Blue symbols are those points used in the final fit; green symbols are those identified as outliers, most of which are attributed to uncorrelated coincident excitations.

or quality of imagery. The main disadvantage of the particle excitations as a crosstalk diagnostic is the very low frequency of events, particularly at the high end of the signal range. A single lunar calibration provides better overall coverage to characterize crosstalk in the Terra NIR bands than 20 months of cumulative particle excitation data even in the best cases. The LWIR band detectors, which have the most significant crosstalk on Terra MODIS, do not even register enough events of sufficient magnitude to perform a basic analysis.

In addition to evaluating crosstalk, further analysis of the particle excitation statistics could also be used to quantify any direct negative impact of these events on the Earth scene imagery, particularly at the low signal level where the events are more frequent. Though we expect that this is not a real concern, having a methodology to quantify the impacts on orbit for MODIS and VIIRS, or other Earth remote sensing instruments, could be useful.

ACKNOWLEDGMENTS

We are thankful to Junqiang Sun for his technical review of this work.

REFERENCES

[1] Xiong, X., Butler, J., Cao, C., and Wu, X., "Optical Sensors—VIS/NIR/SWIR," in [*Comprehensive Remote Sensing*], 353–375, Elsevier (2018).

[2] Lee, T. E., Miller, S. D., Turk, F. J., Schueler, C., Julian, R., Deyo, S., Dills, P., and Wang, S., "The NPOESS VIIRS Day/Night Visible Sensor," *Bulletin of the American Meteorological Society* **87**, 191–200 (Feb. 2006).

[3] Wilson, T., Wu, A., Shrestha, A., Geng, X., Wang, Z., Moeller, C., Frey, R., and Xiong, X., "Development and Implementation of an Electronic Crosstalk Correction for Bands 27–30 in Terra MODIS Collection 6," *Remote Sensing* **9**, 569 (June 2017).

[4] Sun, J., Xiong, X., Madhavan, S., and Wenny, B. N., "Terra MODIS Band 27 Electronic Crosstalk Effect and Its Removal," *IEEE Transactions on Geoscience and Remote Sensing* **52**, 1551–1561 (Mar. 2014).

[5] Sun, J., Xiong, X., Li, Y., Madhavan, S., Wu, A., and Wenny, B. N., "Evaluation of Radiometric Improvements With Electronic Crosstalk Correction for Terra MODIS Band 27," *IEEE Transactions on Geoscience and Remote Sensing* **52**, 6497–6507 (Oct. 2014).

[6] Wilson, T. M. and Xiong, X., "Electronic crosstalk characterization and correction for MODIS bands 1 and 2 using lunar observations," in [*Proceedings of SPIE*], **11127**, 111271X (Sept. 2019).

[7] Keller, G. R., Wilson, T., Geng, X., Wu, A., Wang, Z., and Xiong, X., "Aqua MODIS Electronic Crosstalk Survey: Mid-Wave Infrared Bands," *IEEE Transactions on Geoscience and Remote Sensing* **57**, 1684–1697 (Mar. 2019).

[8] Sun, J. and Wang, M., "Crosstalk Effect in SNPP VIIRS," *Remote Sensing* **9**, 344 (Apr. 2017).

[9] Link, D. O., Aldoretta, E. J., Wilson, T., and Xiong, X., "Measuring crosstalk in MODIS spectral bands on-orbit using the SRCA," in [*Proceedings of SPIE*], **11501**, 115010E (Aug. 2020).

[10] Seppälä, A., Verronen, P. T., Sofieva, V. F., Tamminen, J., Kyrölä, E., Rodger, C. J., and Clilverd, M. A., "Destruction of the tertiary ozone maximum during a solar proton event," *Geophysical Research Letters* **33**(7), L07804 (2006).

[11] Verronen, P. T., Seppälä, A., Kyrölä, E., Tamminen, J., Pickett, H. M., and Turunen, E., "Production of odd hydrogen in the mesosphere during the January 2005 solar proton event," *Geophysical Research Letters* **33**, L24811 (Dec. 2006).

[12] Stassinopoulos, E. and Raymond, J., "The space radiation environment for electronics," *Proceedings of the IEEE* **76**, 1423–1442 (Nov. 1988).

[13] Panasyuk, M., Kalegaev, V., Miroshnichenko, L., Kuznetsov, N., Nymmik, R., Popova, H., Yushkov, B., and Benghin, V., "Near-Earth Radiation Environment for Extreme Solar and Geomagnetic Conditions," in [*Extreme Events in Geospace*], 349–372, Elsevier (2018).

[14] Ziegler, J., Biersack, J., and Ziegler, M., "SRIM—The Stopping and Range of Ions in Matter (SRIM Co., 2008)," *www.srim.org* .

[15] Barnes, W., Pagano, T., and Salomonson, V., "Prelaunch characteristics of the Moderate Resolution Imaging Spectroradiometer (MODIS) on EOS-AM1," *IEEE Transactions on Geoscience and Remote Sensing* **36**, 1088–1100 (July 1998).

[16] Xiong, X., Chiang, K.-F., Adimi, F., Li, W., Yatagai, H., and Barnes, W. L., "MODIS correction algorithm for out-of-band response in the short-wave IR bands," in [*Proceedings of SPIE*], **5234**, 605 (Feb. 2004).